P2-15-03

Liposomal Annamycin Inhibition of Lung Localized Breast Cancer

Rafal Zielinski, Krzysztof Grela, Stanislaw Skora, Izabela Fokt, Matthew Sander, Adam Didluch and Waldemar Priebe

Department of Experimental Therapeutics, UT MD Anderson Cancer Center, Houston TX

San Antonio Breast Cancer Symposium®
December 10-14, 2019

THE UNIVERSITY OF TEXAS MD Anderson Cancer Center
Making Cancer History®

Introduction

Annamycin (ANN) is a non-cardiotoxic anthracycline antibiotic with unique biological properties. It has been formulated in liposomes (L-ANN) and is currently in clinical studies in AML patients. Our earlier studies showed that ANN is not cross-resistant with doxorubicin (DOX) and is a poor substrate for P-glycoprotein 1 (P-gp) [aka ATP-binding cassette sub-family B member 1 (ABCB1)] or multidrug resistance protein 1 (MDR1)], a major mechanism of DOX resistance in different types of cancer [1]. ANN, in contrast to DOX, achieves relatively high levels of cellular accumulation, especially in multidrug resistant (MDR) cell lines, and induces significant DNA damage in cancer cells including MDR cells. In vivo activity of L-ANN has been confirmed in different tumor models. Importantly, in contrast to DOX, Annamycin showed significantly lower cardiotoxicity [1]. Surprisingly, pharmacokinetic and organ distribution studies of ANN and L-ANN revealed disproportionately high drug levels in lung tissue. Annamycin levels (AUC, 24 h) in lungs were over 10-fold greater than in plasma, resulting in levels exceeding those of DOX 6 to 7-fold [2]. This fact has not been considered before as the basis to select a specific clinical indication or patient population for clinical studies of L-ANN. We hypothesize that high levels of ANN in lung tissue will correlate with increased drug efficacy in models of lung localized tumors. The positive results of our in vivo preclinical studies will confirm this hypothesis and support clinical development of L-ANN for treatment of cancers metastatic to lungs.

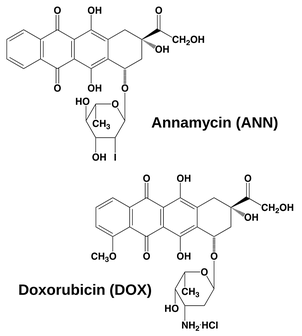

Figure 1. Structure of Doxorubicin and Annamycin

Methods

- Uptake and subcellular distribution of ANN was assessed using confocal microscopy and FACS
- *In vitro* properties of ANN were assessed in triple negative breast cancer (TNBC) 4T1 and/or colon CT26 cells by histone HA2X phosphorylation at S139; and 72 h proliferation assays
- Biodistribution of ANN was tested in naïve CD-1 mice after intravenous administration of the drug
- Efficacy of L-ANN was tested in a syngeneic models of TNBC and colon cancers localized in lungs; immune-competent Balb/c mice were injected intravenously with 4T1 and CT26 cells expressing firefly luciferase.

Results

Uptake and *in vitro* activity of Annamycin

ANN shows rapid and dose-dependent accumulation inside cells, with significantly higher rate of uptake than DOX (Fig. 2A). Immunofluorescent imaging shows significantly different subcellular distribution pattern when compared to DOX (Fig. 2B). Based on HA2X phosphorylation, exposure to ANN results in time-dependent accumulation of DNA breaks (Fig. 2C and 2D) and induction of cell cycle arrest and apoptosis. IC50 values for ANN (72h exposure) are in low nanomolar range and generally 2-10 times lower than for DOX.

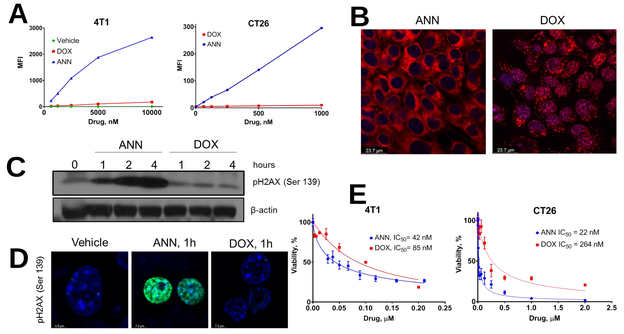

Figure 2. Uptake, subcellular distribution, and cytotoxicity of Annamycin (ANN) in cancer cells

(**A**) Uptake of ANN by 4T1 and CT26 cells measured by FACS; **(B)** Subcellular distribution of ANN and DOX in 4T1 cells; **(C-D)** Double Strand Break (DSB) formation and apoptosis induction detected by H2AX (Ser139) analyzed by Western blot (WB) or fluorescent microscopy; **(E)** 72h toxicity of ANN and DOX in 4T1 and CT26 cells.

Pharmacokinetics and organ distribution

The highest concentration of ANN after intravenous administration measured in lungs was 138 μg/ml (216 μM), nearly ten times higher than C max measured for ANN in plasma. Significant amounts of drug were also detected in the spleen (Fig. 3)

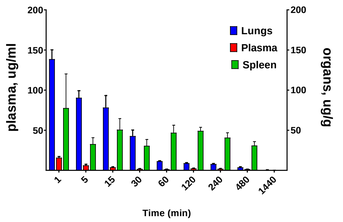

Parameter	Units	Estimate		
		Plasma	*Lung*	*Spleen*
$T_{1/2}$	min	314	282	548
T_{max}	min	1.00	1.00	1.00
C_{max}	μg/mL (μg/g)	15.9	138.7	77.7
AUC_{last}	min*μg/mL (min*μg/g)	1569	7417	19302

Figure 3. Pharmacokinetic and organ distribution of ANN after intravenous administration

CD-1 mice (n=5-8) were dosed with L-ANN 4 mg/kg, followed by exsanguination at nine time points. Plasma and selected organs were isolated. ANN levels in plasma and organs tissues were measured using LC-MS/MS

Efficacy of L-ANN in 4T1 TNBC "lung metastasis" model

L-ANN showed remarkable inhibition of metastatic growth of lung localized 4T1 cells after two doses of the drug (Fig. 4A-4D). Interestingly, the vehicle-group developed pronounced splenomegaly, while L-ANN treated mice had spleens within normal range (Fig. 4E). Further extension of survival was achieved in experiments where mice were dosed once a week for six weeks. The median survival of treated group increased to 56 days vs 23 for vehicle (p<0.0001 Fig. 4F).

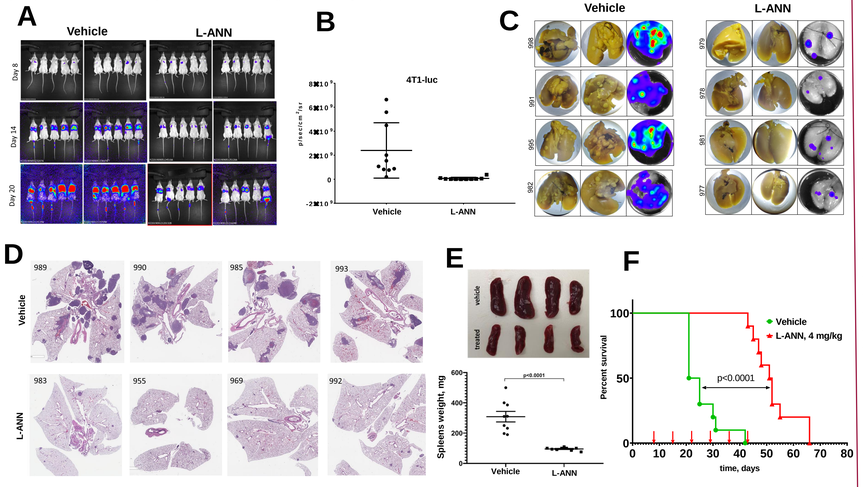

Figure 4. Efficacy of L-ANN in 4T1 TNBC "lung metastasis" model.

Female Balb/c mice were injected with 2 x 10^4 4T1-Luc cells through tail vein injection. Eight days after tumor cell inoculation, mice were injected with L-ANN at 4 mg/kg or saline. **(A)** Bioluminescent images of mice after two doses of L-ANN. **(B)** distribution of bioluminescent signal in vehicle or L-ANN-treated mice. **(C)** Microscopic image of Bouin solution-stained lungs after two doses of L-ANN and vehicle along with corresponding BLI. **(D)** H&E stained lung sections. **(E)** Spleens extracted from vehicle- or L-ANN treated mice and their weight distribution (p value based on two-tailed Student's t-test). **(F)** Survival curves of 4T1-luc injected mice receiving six doses of L-ANN (4 mg/kg) or vehicle on a once a week schedule. Arrows represent L-ANN injection.

Efficacy of L-ANN in CT26 colon cancer "lung metastasis" model

Remarkable response to L-ANN was also recorded for mice bearing lung colonized CT26 colon cancer. Significant inhibition of tumor growth was observed after the first injected dose (Fig. 5A and B). Figure 5C shows CT image on vehicle- and L-ANN-treated (6 mg/kg) mice performed on day 25. Figure 5D is a representation of bioluminescent and microscopic images of extracted lungs. Continuous treatment led to significant extension of survival (median survival for vehicle was 22 days and has not been reached for treated groups, Fig. 5B).

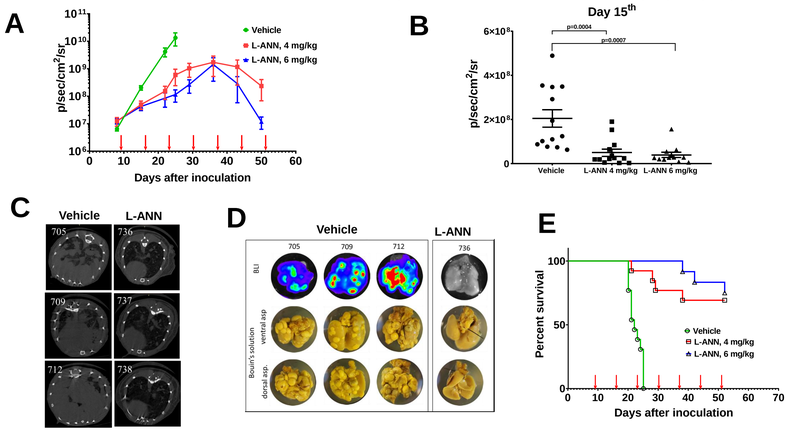

Figure 5. Efficacy of L-ANN in CT26 colon cancer "lung metastasis" model

Female Balb/c mice were intravenously injected with 2x10^5 CT26.WT-Luc-neo cells. Nine days after tumor inoculation mice were randomized into three groups receiving vehicle (saline), L-ANN at 4 mg/kg or 6 mg/kg. (**A-B**) Longitudinal analysis of BLI signals and. Its distribution 7 days after first dose of L-Ann (**C**) Axial CT image of mice receiving vehicle or L-ANN 6 mg/kg performed on day 25) **(D)** BLI and microscopic images of extracted lungs fixed with Bouin's solution. Survival curves of vehicle and L-ANN treated mice. Arrows represent L-ANN injection

Summary

- ANN is a potent anticancer agent inducing DNA damage and shows nanomolar efficacy against tested cancer cells
- ANN shows dose- and time-dependent accumulation in cells with increased cytosolic localization as compared to DOX
- L-ANN, liposomal formulation of ANN has been developed and currently is being evaluated in clinical trials in AML patients
- PK and biodistribution studies in mice show high levels of ANN in lungs with a peak concentration reaching 200 μM
- L-ANN significantly inhibits tumor growth of lung-localized breast and colon cancers
- L-ANN reduces splenomegaly in tumor bearing animals
- L-ANN significantly extends survival and reduces tumor burden in mice with advanced lung localized cancers

Reference

1. Priebe W, Perez-Soler R. Design and tumor targeting of anthracyclines able to overcome multidrug resistance: a double-advantage approach. Pharmacol Ther. 1993;60(2):215-34.
2. Zou Y, Priebe W, Stephens LC, Perez-Soler R. Preclinical toxicity of liposome-incorporated Annamycin: selective bone marrow toxicity with lack of cardiotoxicity. Clin Cancer Res. 1995;1(11):1369-74.

Acknowledgments and Disclosures

We would like to thank Dr. Mihai Gagea Iurascu for help in histopathology analysis.
This work was supported by a grant from Moleculin Biotech, Inc. (NASDAQ: MBRX).
Dr. Waldemar Priebe is Chairman of the Scientific Advisory Board and owns stock in Moleculin Biotech, Inc.
Please contact us at wpriebe@mdanderson.org for permission to reprint and/or distribute this presentation.